This article has been accepted for publication in IEEE Transactions on Communications. This is the author's version which has not been fully edited and content may change prior to final publication. Citation information: DOI 10.1109/TCOMM.2022.3190424

Experimental demonstration of multigigabit data communication using surface waves on twisted-pair cables

Ilana Toledano, Syed Bukhari, Ahmed Aziz, Ergin Dinc, Tobias Schaich, Daniel Molnar, Anas Al Rawi, Eloy de Lera Acedo, Michael Crisp and Richard Penty

***Abstract*—The demand for higher broadband speeds is ever increasing whereas the deployment of full fibre to the premises is slower than initially predicted and remains costly. Solutions exploiting the existing, ubiquitous, copper network and increasing its capacity would be highly beneficial in the near term. One approach is to use surface wave (SW) transmission mode to transmit signals over the existing copper cabling network. We present proof-of-concept experimental SW data transmission on twisted pair cables. A surface wave launcher for low GHz carrier frequency operation is designed and optimised. Experimentally, we demonstrate data rates in excess of 12 Gb/s in a 1.15-3.25 GHz band over a 6.1 m twisted pair cable with an average bit error rate of 2.25×10^{-5}, without coding or feedback implementation. Furthermore, higher frequency bands are tested with data rates up to 3.4 Gb/s displaying their potential for surface wave transmission. S-parameter measurements allow capacity estimations of SW data transmission on longer cable lengths using water-filling algorithms. Our calculations predict over 13 Gb/s capacity on a 100 m cable using a 3.5 GHz transmission bandwidth, this may be further extended by further increases to the bandwidth used for SW transmission.**

***Index Terms*—Wired Communication, Surface Waves, Twisted Pair Cables, DSL Technologies, Data Communication, Goubau Line, Surface Wave Launcher, Planar Launcher**

I. INTRODUCTION

Surface waves (SW) for data transmission have long been a subject of interest since their use as an antenna for television broadcasting [1]. Surface waves were discovered in 1899 by Sommerfeld [2] as a solution to Maxwell's equations where the electromagnetic (EM) wave is transmitted as the TM_{01} mode on a single wire with finite conductance, resulting in very low attenuation and low phase dispersion over very wide bandwidth even at high carrier frequencies. However, surface waves also suffer from a large field extent at lower frequencies. Later, Goubau discovered that if the conductor's surface was modified, either corrugated (spoof surface plasmon) or coated with a dielectric (often called G-line), the field could be more confined to the surface of the wire with losses remaining low. These characteristics make the technology well suited for high-speed data transmission [3]. For this reason, some attention has been given to the use of this technology in modern telecommunication systems, either for terahertz photonically generated systems [4] [5] or more recently reusing the existing copper cable access network infrastructure, such as AT&T with the AirGig project [6] and Cioffi leading the new field of TDSL using vectoring [7]–[9]. Much literature has covered experimental surface wave links' frequency response, antenna design [10] and theoretical calculation [11]–[14], but very little has reported experimental data transmission [15]–[17]. In this paper, we demonstrate a proof-of-concept setup for wideband orthogonal frequency division multiplexing (OFDM) multigigabit data communication over a Dropwire DW11 (a standard single pair overhead final drop cable deployed extensively in the UK BT network) using surface wave transmission. Shorter cable lengths are used for the experimental study due to practical limitations. The results are extrapolated to longer lengths to allow comparison to existing and widely implemented DSL standards.

This paper is building on Goubau's original work with the aim to provide further insight into the experimental capabilities of surface waves. A low-GHz band is used as a proof of concept to test a twisted pair line with modern days modulations and data processing for the first time, showing the potential to use higher frequency bands in future work. Furthermore the planar conical horn antenna is tested for surface waves data communications applications. Both experimental and simulated links are then correlated and used to predict the capacity of the link for longer cables and more advanced data processing.

The outline of this paper is as follows. In Section II, we present the experimental setup, the SW launcher design and the data processing used. Section III presents the experimental results. This covers wideband data transmission with bit error rate (BER) measurements, then higher modulation order over narrower bandwidths, with characterisation of the errors and finally measurements of various datasets at higher carrier frequencies. In Section IV, a numerical extrapolation is used to predict surface wave transmission performance for longer cable lengths, which would be a closer match to real application scenarios. Finally, conclusions are drawn in Section V.

II. METHODOLOGY AND EXPERIMENT DESIGN

A. Experiment setup

The experimental data transmission setup is shown in Figure 1. For maximum flexibility, most of the data generation and processing steps are performed in the digital domain which

IT contributed to the data transmission part of the paper and SB to the antenna design part.

IT, SB, AA, DM, TS, MD, MC, ELA, MP are with the University of Cambridge, TM, FB, AAR with BT. Since the research was conducted AAR moved to Ofcom, and ED has moved to Isotropic Systems

This article has been accepted for publication in IEEE Transactions on Communications. This is the author's version which has not been fully edited and content may change prior to final publication. Citation information: DOI 10.1109/TCOMM.2022.3190424

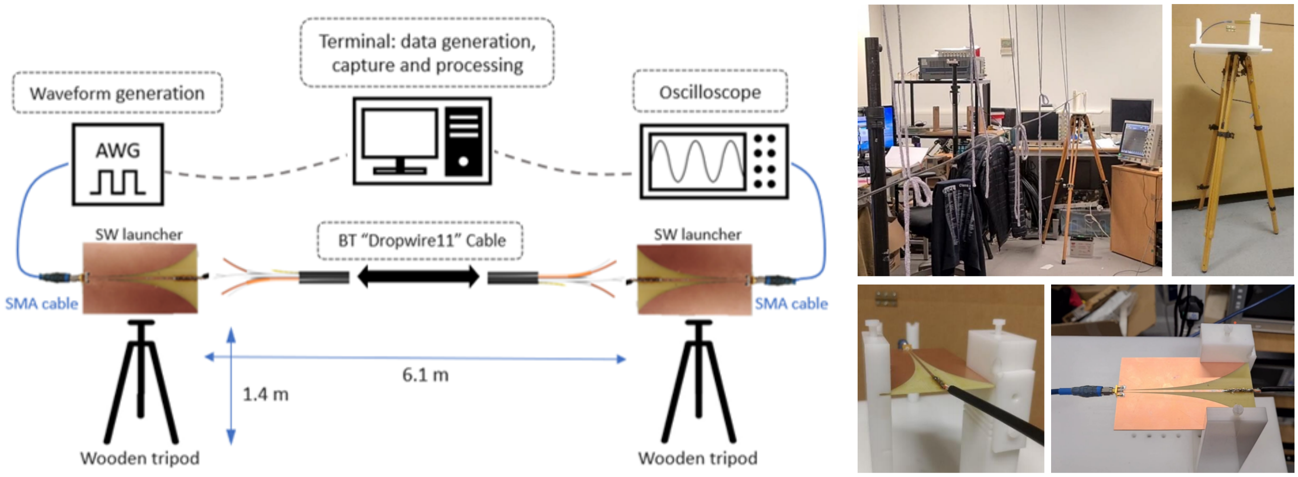

Fig. 1. Diagram and pictures of the surface wave data transmission lab setup including the lab equipment, the full surface wave link and the computer where data generation, capture and processing takes place

also minimises analogue domain errors and impairments. The transmission link consists of launchers which convert the coaxial TEM mode of the test and measurement equipment into the surface wave for transmission on the DW11 cable. The launchers are described in detail in Section II-B. The DW11 cable is suspended in free space and maintained as straight as possible.

Most surface wave theory considers surface waves on a cylindrical medium giving rise to a circular H-field and a, primarily, radial E-field component. In our experiments we study a more complex cable (BT DW11 cable [18]) representative of deployed overhead cables networks. The cable consists of a single copper twisted pair with polyethylene coating, 3 steel strength members coated with PVC and a nylon ripcord all bundled in a medium density polyethylene sheath of about 5.4 mm outer diameter, a theoretical study of surface waves over this cable can be found in [19]. Due to the large field extent of the surface wave, the cable cannot be wound on a drum to facilitate long cable tests in a restricted space. Hence the cable length was 6.1 m from launcher to launcher, limited by the laboratory size.

Due to the field extent of the surface wave and to reduce dependence of the results on the environmental surroundings, the launchers were positioned above the ground using wooden tripods. To reduce attenuation from bends and irregularities [20], the cable was supported at regular intervals with nylon wool suspension supports which had no measurable impact on the transmission.

The wires (twisted pair and 3 steel strength members) were all soldered together and to the surface wave launchers which were held by plastic supports designed to have minimal effect on the performance of the launcher as shown in the pictures Figure 1 and hence minimal launching loss.

Transmitted signals were generated by an arbitrary waveform generator (AWG), with a maximum sample rate of 50 GS/s (Tektronix 70001A [21]). On the receiver side, a digital storage oscilloscope (DSO) was used, with up to 20 GS/s sampling rate and 8 GHz bandwidth (Teledyne LeCroy WavePro 804HD [22]). A computer was used to initiate the AWG transmission and capture the DSO time series. Further processing of the time series yields the results presented.

B. The surface wave launcher

A methodical process for integrating and designing surface wave launchers for communication systems has been developed. Due to ease of fabrication, and therefore its low cost, a planar surface wave launcher compatible with standard printed circuit board (PCB) processes is developed. Planar launchers for terahertz [10] [23] and microwave frequencies [24] have been presented. The microwave launcher has identical top and bottom metallic layers whose geometry is inspired from Vivaldi antennas and a bandwidth of 1.4GHz.

Our launcher is single-sided, utilizes a coplanar waveguide (CPW) and operates over a multigigahertz bandwidth. A wide bandwidth is acheived based on the concept of gradual impedance transformation. We hypothesize that a single conductor carrying surface waves is equivalent to a coaxial cable for which the outer condctor is a thin shell with an infinite radius. This assumption is only valid when the dielectric and metallic losses are present in the system. (It is important because in the case of a Sommerfeld wave where there are no metallic and dielectric losses, fields can extend to an infinite distance [3]).

1) Surface wave launcher design: To design an efficient SW launcher our goal is to match the impedance of a CPW to that of the SW carrying conductor. Since we assume the SW carrying conductor to be akin to a CPW with its ground plane at infinity, we gradually taper the CPW ground plane in order to minimize the reflections arising due to the impedance mismatch. We employ an exponential taper using the continuous exponential function. This reduces reflections which can arise due to impedance mismatch and yields a wideband response from the launcher. It should be noted that the SW operates in TM_{01} mode while a CPW (and coax) are operating in TEM mode. In order to make this transition efficient the fields at the edge of the launcher should resemble

This article has been accepted for publication in IEEE Transactions on Communications. This is the author's version which has not been fully edited and content may change prior to final publication. Citation information: DOI 10.1109/TCOMM.2022.3190424

those of the SW [5]. This is implicit in our design because the SW fields are concentrated around the SW conductor similar to the fields of a CPW at the edge of the launcher.

We illustrate and validate our design process with simulations using CST Microwave Studio. The template of the launcher design and the simulation setup is illustrated in Figure 2 (a). The initial impedance of the CPW is 50 Ω and the centre copper trace is 2.5 mm wide. The ground plane is tapered along the y-axis according to a function e^{ay}, where a is the tapering parameter with a value of 0.04. The dielectric material forming the base of the CPW has a relative permittivity of 3 and a loss tangent of 0.02. The width of this dielectric slab is kept at 60 mm. The parameter s measures the cross-sectional distance between the ground planes (secondary conductor) at the edge of the launcher. Due to the exponential taper, increasing this distance requires an increased length of the launcher. The results of simulations for 3 different launchers of length 20, 40 and 80 mm are shown in Figure 2 (b). The value of s for these launchers is 5.5 mm, 10 mm, and 50 mm, respectively. As s increases, the reflection and transmission response of the launcher improves (for s= 50 mm, reflections are below -10 dB for almost the entire frequency band therefore illustrating a multiGHz wideband response; the transmission also improves with increasing s).

To demonstrate the importance of gradual tapering (and gradual impedance change), the value of s is kept constant at 50 mm and launchers with different tapering parameters are compared, in Figure 3. It is clear from this figure that the response of the launcher considerably deteriorates when the tapering parameter is increased from 0.04 to 0.4. This can be explained in terms of characteristic impedances. Equation (1) provides an estimate of the characteristic impedance, Z_0, of a CPW [25].

$$Z_0 = \frac{30\pi K(t')}{\sqrt{\varepsilon_{eff}}K(t)} \tag{1}$$

where K is the elliptic integral of first kind, $t' = \sqrt{1-t^2}$ and $t = \frac{w}{w+2s}$, such that w is the width of the centre conductor, $\varepsilon_{eff} = \frac{1+\varepsilon_r}{2}$ and s is the distance between the centre conductor and the ground.

This equation indicates that as s increases, impedance also increases, so a longer tapering parameter leads to a faster change of impedance, resulting in larger reflections and reduced transmission; Figure 3 demonstrates the manifestation of this phenomenon. We also investigated the effects of changing the radius of the copper wire connecting the two launchers but no significant change in the transmission and reflection response was observed.

2) Experimental Validation: Fabricated SW launchers are shown in Figure 1. These prototype launchers were designed and fabricated on an FR4 material ($\epsilon_r = 4.3$ and $tan\delta = 0.025$). We selected the tapering parameter to be 0.03 in order to maximize the wideband characteristics of the launchers. The launchers were 12 cm in length and 8cm in width. The centre conductor was 2.5 mm wide and the separation between the ground planes (at the edge of the launcher) s was 75 mm. For initial characterisation, two launchers were connected with a 2.5 mm copper trace printed on the FR4 substrate to act as a surface wave transmission line. An excellent agreement between the measurements and simulations was recorded and is shown in Figure 4. The S11 reflection characteristics (of both launchers) over the whole band remain below -10 dB, demonstrating wideband performance. S21 transmission response over the whole band is also very good, falling approximately with frequency. S-parameters with no wire between the two launchers has been measured experimentally resulting in

(a)

(b)

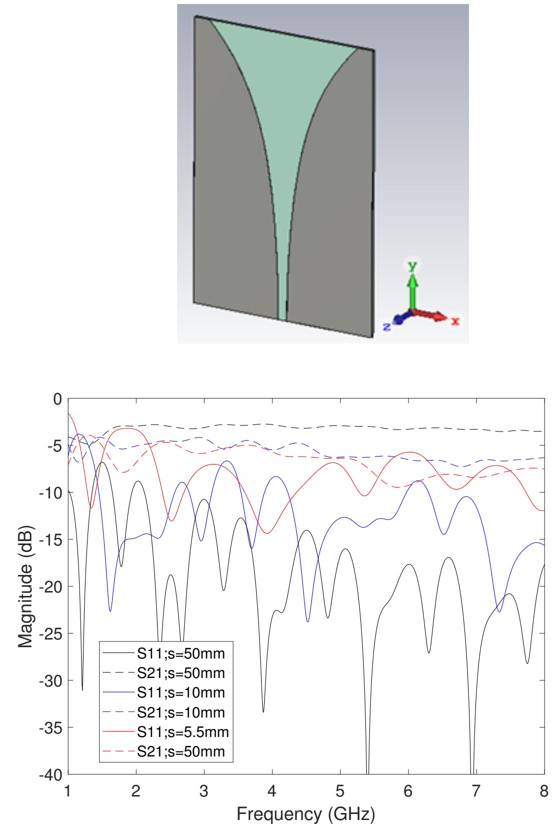

Fig. 2. (a) Schematic diagram of the simulated launcher (b) Effect of the length/ground plane gap on the Transmission and reflection characteristics of the launcher

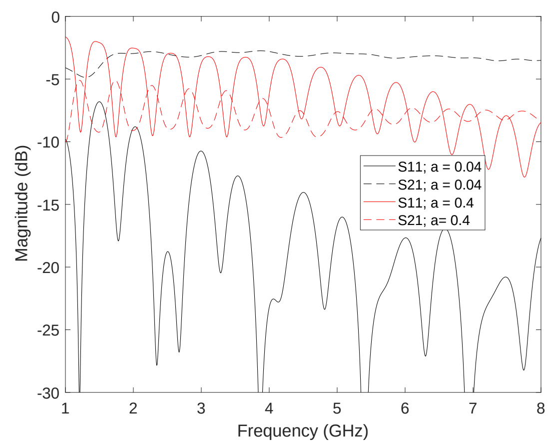

Fig. 3. Effect of tapering/gradual impedance transformation on the reflection and transmission characteristics of the launcher

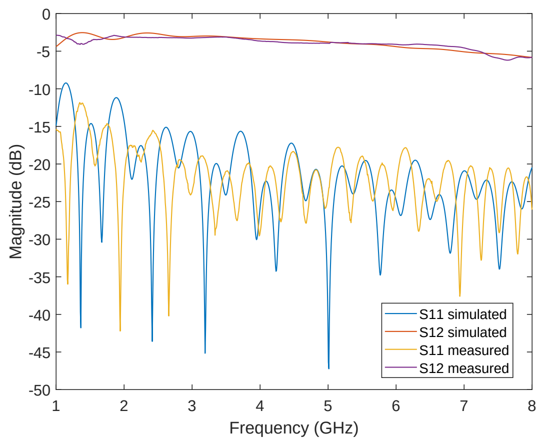

Fig. 4. Measured and simulated comparison of transmission (S21) and reflection (S11) characteristics of SW launchers

no transmission (very low S21 and high S11) similar to [10].

These launchers were then utilised to perform measurements over a 6.1 m-long DW11 wire as shown in Figure 1. The frequency response is displayed in Figure 5. The higher attenuation than in Figure 4 is due to the longer wire length and the more complex structure of DW11. Furthermore, a large transmission notch (very lossy) region is observed from about 3.5 to 4.2 GHz. This notch is the result of the DW11 cable structure, and further detail about the origin of this behaviour can be found in our theoretical paper [19]. However, surface wave transmission over this cable presents two good transmission windows, between 1 and 3.5 GHz and 4.5 to 6.5 GHz with an average transmission loss of 6.9 dB and 14.5 dB respectively.

C. Data generation and processing

For data transmission a modulated OFDM waveform is generated in MATLAB. The block diagram in the top of Figure 6 illustrates the generation steps and parameters for a single frame. A random bit sequence is generated, and modulated by an M-order QAM modulator with Gray coding. The modulated symbols are then passed to the OFDM modulator where the data is converted from serial to parallel, undergoes an inverse discrete Fourier transform to translate from the frequency to the time domain, and is converted back to a serial data stream. Finally, a cyclic prefix (CP) is added at the front of each OFDM symbol [26]. (In the following experiments, the cyclic prefix length was chosen as 1/32 of the number of sub-carriers.)

A preamble is added at the beginning of the frame following Schmidl & Cox's preamble design [27]. Pulse shaping (raised root cosine, span = 10 and roll-off = 0.22) filtering and oversampling are applied to allow numerical mixing to a chosen carrier frequency, f_c, and obtain a passband signal of bandwidth BW.

The data recovery and processing are essentially the same process in reverse as shown at the bottom of Figure 6. First the low frequency and DC components are removed, then the data is resampled from the DSO sampling frequency to the

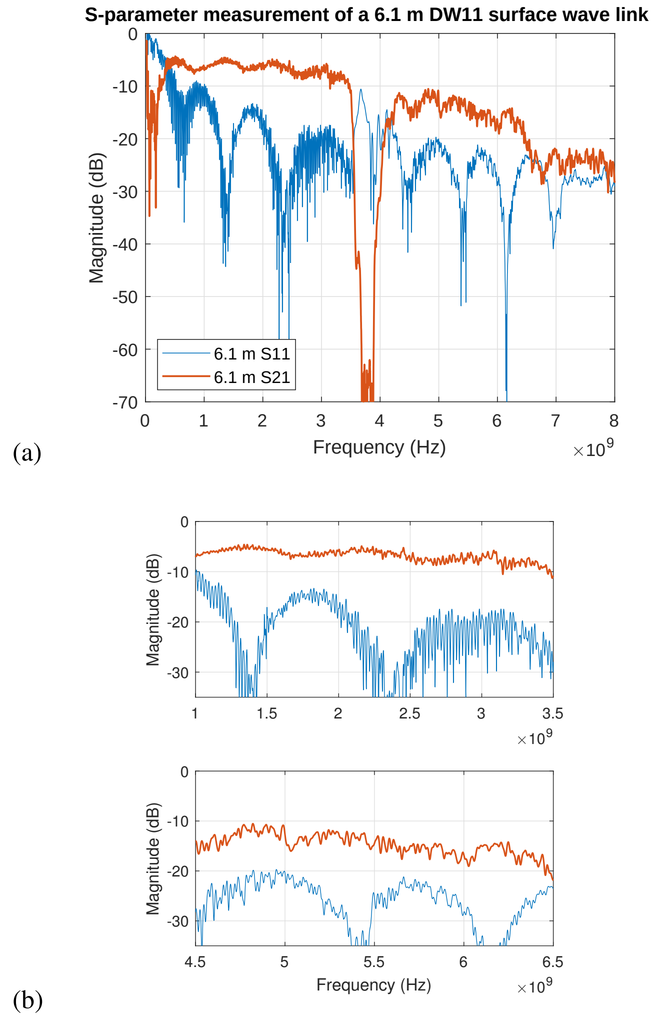

Fig. 5. (a) S-parameters of the DW11 surface wave link presented in Figure 1 (b) enlargement of the response of the two transmission frequency bands (1-3.5 and 4.5-6.5 GHz)

original AWG's sampling frequency and converted to complex baseband IQ samples. Using the preamble, the start of the signal is detected (following [27]) resulting in coarse timing recovery. For fine timing recovery, the known preamble's cyclic prefix is located within the coarse preamble start range.

The data is down sampled to the Nyquist rate and OFDM demodulated; firstly removing the cyclic prefix, and applying a Fourier transform, resulting in serial QAM symbols in the frequency domain, where the channel effect can clearly be observed.

At this point, a single tap equaliser, calculated from channel estimation, is used to recover the expected QAM signal. The channel is estimated using the first symbol of the sequence which directly follows the preamble (assumed to be known at the receiver side), with the following equation:

$$H_{est}\left(f_{subcarrier}\right) = \frac{QAM_{Rx}(f_{subcarrier})}{QAM_{Tx}(f_{subcarrier})} \quad (2)$$

With H_{est}, the complex channel response at each subcarrier and QAM_{Rx} and QAM_{Tx}, the value of the QAM data (complex value) received and transmitted at each subcarrier

This article has been accepted for publication in IEEE Transactions on Communications. This is the author's version which has not been fully edited and content may change prior to final publication. Citation information: DOI 10.1109/TCOMM.2022.3190424

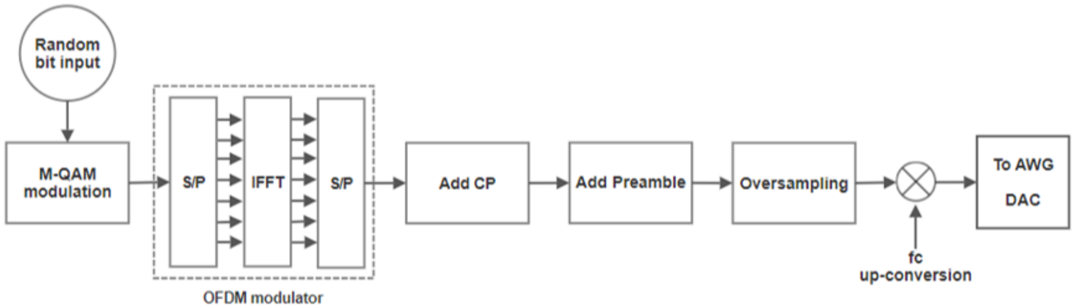

(a)

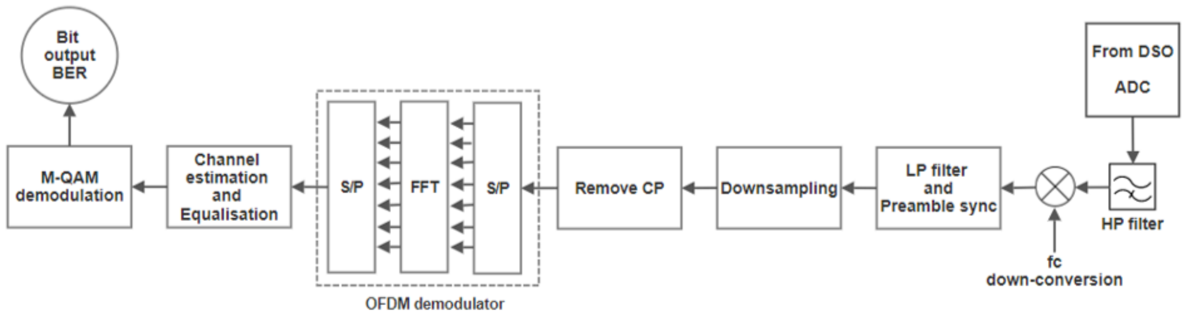

(b)

Fig. 6. (a) Data generation and (b) processing block diagrams

frequency, $f_{subcarrier}$.

Further processing is performed on the raw channel estimate to remove noise and better approximate the overall response of the full frame. Outlying points were removed from the initial H_{est} using MATLAB's built-in function, and smoothing was applied by taking a moving average with a chosen window generally equal to 10 subcarriers. The data symbols were equalised using the smoothed channel estimate, hence an equalised QAM sequence was obtained and demodulated to recover the bit stream and bit error rate.

The overhead, OH, in this data transmission can be calculated as follows:

$$OH = \left(1 - \frac{sym_{known}}{sym_{tot}}\right)\left(1 - \frac{CP}{subcar + CP - nulls}\right) \quad (3)$$

Where sym is the number of OFDM symbols defined by their suffix and $subcar$, CP, $nulls$, the number of subcarriers, cyclic prefix length and number of nulls within one OFDM symbol.

It is worth noting that neither bit loading nor forward error coding (or other data coding) were implemented though, we note that both would likely increase the system performance.

III. Data transmission results

The main objective of this experiment is to demonstrate that surface waves can achieve data capacities beyond current copper access data transmission standards on the same cables. We compare to G.fast which acheives 1-2 Gb/s over distances of up to 100 m on twisted pair bundles [28]. Our setup was limited by the laboratory dimensions of just over 6 metres, but it can be estimated that the data rate and transmission length have an inverse relationship. So, to achieve over 1 Gb/s over a 50-100 m range, a performance beyond 10 Gb/s on a 5-10 m link is required.

A. 12.5 Gb/s pre overhead - 64-QAM data transmission

1) Single frame transmission: In the first case, a data rate of 12.5 Gb/s (pre-overhead) was transmitted. The data set occupied a 2083 MHz bandwidth with 64-QAM modulation and a carrier frequency of 2.1 GHz (1.06 to 3.14 GHz). The dataset was composed of 1 frame of 20 OFDM symbols each divided into 2048 subcarriers (including 2 nulls at 1.58 GHz). Once the data was synchronised using the preamble (Figure 7 (b)), the single frame was demodulated and the first OFDM symbol was used to obtain a channel response estimate (Figure 7 (c)) for the single tap equaliser.

TABLE I
Parameters' summary of the two BER test datasets

Modulation	64-QAM
Bandwidth	2083.33 MHz
Carrier frequency	2.1 GHz
DR (pre overhead)	12.5 Gb/s
Subcarriers	2048
Subcarriers bandwidth	1017.25 MHz
Frames	20
Symbols	20 or 50
Nulls	0 or 76
Samples per symbol	6
AWG signal power	-10.4 dBm

The corrected signal constellation is shown in Figure 7 (d), the squares represent the hard decision thresholds of the QAM symbols. It can be seen that the signal is well equalised and the resulting QAM data is close to the expected values; some points are slightly scattered but remain within the error margin. The EVM of the successive symbols remains stable over the equalised frame. For this specific dataset, 0 errors were recorded for a total of 233244 data bits sent, this was

This article has been accepted for publication in IEEE Transactions on Communications. This is the author's version which has not been fully edited and content may change prior to final publication. Citation information: DOI 10.1109/TCOMM.2022.3190424

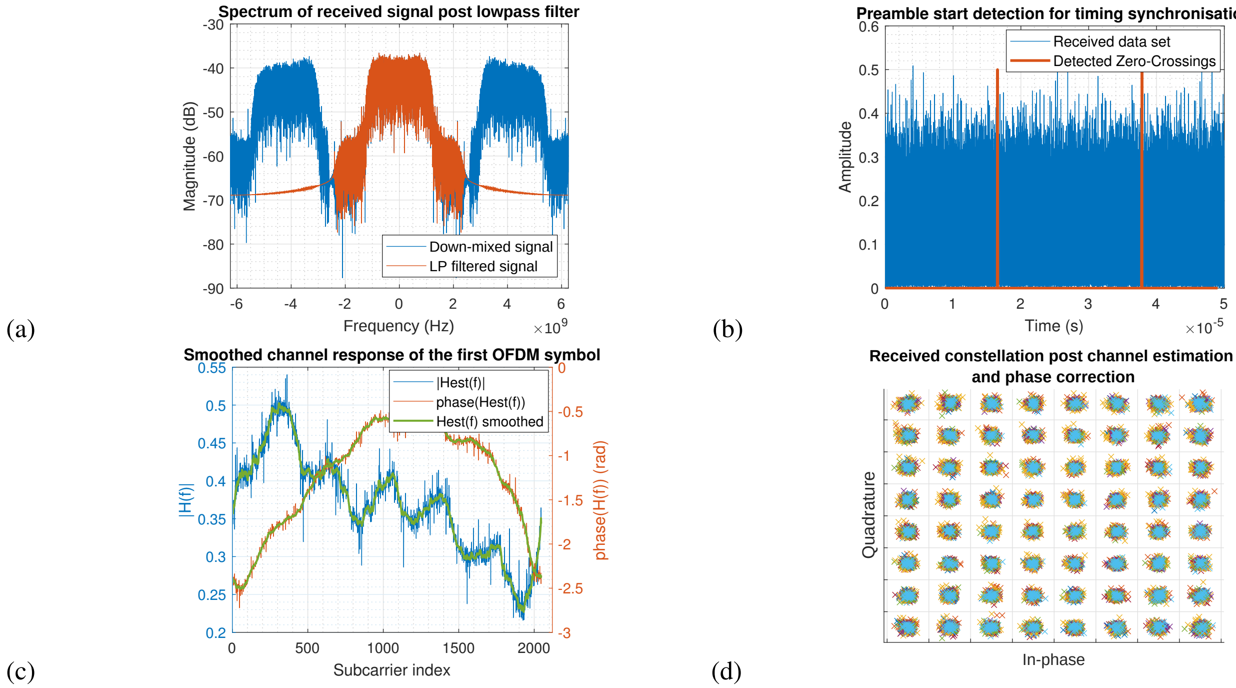

Fig. 7. Results obtained from the 64-QAM data processing, (a) Captured baseband spectrum (b) Preamble start detection on the time domain signal, indicated by each orange peak (c) Channel phase and magnitude estimation and corrections of the frame's first symbol (d) Constellation of the equalised frame, each colour representing a different OFDM symbol

representative of the other datasets recorded for single frame data transmission at 2.1 GHz (1 or more errors would have resulted in an overall BER $> 4.3 \times 10^{-6}$). The average EVM is 2.97 % with a post overhead throughput of 10.97 Gb/s.

2) Bit error rate measurement: Error-free data transmission beyond 10 Gb/s was demonstrated over a 6.1 m link using relatively short datasets which limit the minimum measurable BER. To obtain a more accurate BER evaluation, the data generation was modified to generate multiple frames. A single data set of 20 frames each containing 20 or 50 symbols and 1 preamble was generated, the latter included nulls over the full 2.4 GHz Wi-Fi band. The minimum measurable BER in these cases are 2.04×10^{-7} or 8.46×10^{-8} with corresponding post-overhead data rates of 12.06 and 12.08 Gb/s (due to a reduced overhead).

The detailed parameters of the experimental data generated for the BER measurements are summarised in Table I. The following Table II contains the exact results, EVM, number of errors and frequency of the detected errors for both data sets which were each repeated 5 times.

The average BER across all 10 measurements is 2.25×10^{-5}. Even though this value is high compared to the current DSL standards which require a BER $< 10^{-7}$ [29], no bit coding, forward error correction or feedback channel detection and bit allocation have been implemented which would allow further BER reduction [30]. The main source of errors was likely due to poor channel performance over narrow frequency bands and interference and is further characterised in section III-C.

TABLE II
DETAILED RESULTS OF THE BER EXPERIMENT

Dataset	Symbols in 1 frame	Frames	Nulls per subcarrier	Total EVM	Errors number	BER	Frequency of error subcarriers
				%			GHz
1	20	20	0	2.46	0	0.00E+00	NA
1	20	20	0	2.61	0	0.00E+00	NA
1	20	20	0	2.83	384	7.83E-05	1.061 & 1.960-1.964
1	20	20	0	2.42	0	0.00E+00	NA
1	20	20	0	2.61	183	3.73E-05	2.403-2.409
2	50	20	76	2.23	0	0.00E+00	NA
2	50	20	76	2.54	0	0.00E+00	NA
2	50	20	76	2.20	0	0.00E+00	NA
2	50	20	76	2.39	584	4.94E-05	2.885-2.890
2	50	20	76	2.39	713	6.04E-05	2.847-2.851

This article has been accepted for publication in IEEE Transactions on Communications. This is the author's version which has not been fully edited and content may change prior to final publication. Citation information: DOI 10.1109/TCOMM.2022.3190424

B. Potential for 256-QAM at different carrier frequencies

As the surface wavelink exhibits multiple passbands, the use of frequency division multiplexing (FDM) could allow multiple users. FDM reduces the required analogue front-end and signal processing bandwidth compared with a wideband solution and can avoid parts of the spectrum [31] where interference may be greater or the channel is poor.

To emulate this data transmission scenario, we transmit three non-overlapping signals at 1.4, 2 and 2.8 GHz each occupying 500 MHz bandwidth. The received spectra post high pass filtering are displayed in Figure 8 (a). The carrier frequencies are chosen to avoid the 2.4 GHz ISM band which was seen to have higher bit errors in previous experiments thought to be caused by interference from nearby Wi-Fi devices.

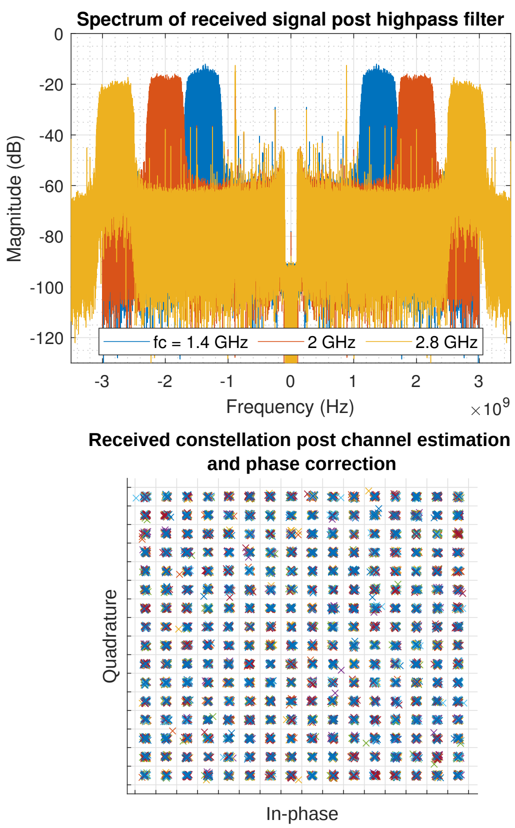

(a)

(b)

Fig. 8. (a) Received spectrum post low-pass filter for multiple 256-QAM data sets of 3 different carrier frequencies, and (b) Post equalisation constellation of the data set at f_c = 1.4 GHz

The data sets were processed as described in the Methodology (section II-A). A representative constellation (f_c = 1.4 GHz) is shown in Figure 8 (b).

A summary of the results is displayed in Table III, the EVMs were all between 1 and 1.5 %, however the results at f_c = 2 GHz are the lowest (best) which could be explained by a better channel response in this band. If transmitted simultaneously, a total of 10.17 Gb/s post overhead throughput is achieved with a 1.5 GHz aggregate bandwidth on the same 6.1 m link as in the previous experiment.

Unlike the previous experiment, the results were less repeatable, with some recurring errors in other data sets.

TABLE III
RESULTS FROM THE RECOVERED DATA FOR 3 SEPARATE 500 MHz 256-QAM SIGNALS OVER A SURFACE WAVE LINK

Dataset	fc	Bandwidth	Total EVM	Datarate post-overhead	Errors
	GHz	MHz	%	Gb/s	
1	1.4	500	1.36	3.39	0
1	2	500	1.02	3.39	0
1	2.8	500	1.39	3.39	0

C. Subcarrier error analysis

Results shown in section III-A were mostly error free (particularly 64-QAM transmission). The errors can be split into two categories: (i) subcarriers with errors over all symbols. These also exhibited a poor H(f) compared to neighbouring subcarriers, so the SNR may have been insufficient for the chosen modulation order, which could be resolved by bit loading with minimal reduction in the overall data capacity; (ii) bursts of errors on particular subcarriers which were not repeatable. It is thought that these are caused by RF interference. In theory surface waves will be insensitive to TEM interference. However, interference in common wireless bands could be seen with a spectrum analyser connected to the surface wave transmission line, thought to be due to the launcher acting as an antenna (at the mode conversion).

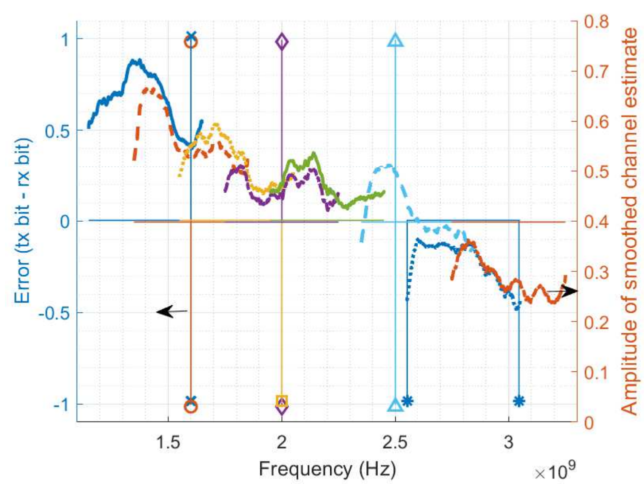

Fig. 9. Frequency response of the channel amplitude (thick lines) and detected errors (thin straight lines with markers) of 256-QAM data transmission at different carrier frequencies (each frequency is represented by a different colour)

To further explore the sources errors, a 256-QAM 500 MHz bandwidth signal was swept over 8 carrier frequencies such that datasets overlapped, to an extent, in the frequency domain. In Figure 9 the channel estimate and resulting errors are plotted against frequency. The channel responses (thick dotted lines) follow the same general trend from one carrier frequency measurement to another, slight oscillations and decreasing amplitude with increasing frequency, but do not match perfectly.

This article has been accepted for publication in IEEE Transactions on Communications. This is the author's version which has not been fully edited and content may change prior to final publication. Citation information: DOI 10.1109/TCOMM.2022.3190424

As for the resulting errors, shown by the thin straight lines with markers at errors, most of the subcarriers with errors occur on the same frequencies irrespective of the carrier frequency and hence position in the ODFM spectrum. The different markers show that fc = 1.6 GHz (circle) has some errors which occur on the same frequencies as fc = 1.4 GHz (cross) and errors at fc = 2 GHz (diamond) match the ones at fc = 1.8 GHz (square). A feedback mechanism could be employed so such frequencies would be either nulled or filled with a lower modulation order symbol, to reduce or eliminate such errors.

In the displayed datasets, the number of errors varies from 0 to 19 out of 114688 transmitted bits giving a BER between 8.72×10^{-6} and 1.66×10^{-4}. The EVM ranges from 1.7 to 2.9 %, averaging at 2.3 %, with EVM increasing with carrier frequency (following the trend of decreasing transmission with frequency). Nevertheless, the carrier frequency with the lowest EVM does not directly correlate with the lowest BER. This suggests that irregularities (especially minima) of the channel response are likely a cause of the recurring errors. The frequency with errors that did not suffer a poor channel was just below 2.5 GHz and is thought to be caused by ISM band interference (Wi-Fi). Furthermore, this experiment has shown the potential to transmit with a high modulation order over a 2.15 GHz wide frequency range.

D. Higher carrier frequency results

The results presented in the previous sections show the potential of the system in the 1-3.2 GHz band, however the overall transmission band of the surface wave does not suffer a theoretical cutoff frequency as seen in other transmission lines. In practice it is limited by the dielectric insulation of the conductor and the design of the launchers. To demonstrate SW data transmission at higher frequencies, tests were carried out between 4.5 and 6 GHz. It should be noted that these results only demonstrate the potential at high frequencies and that the ultimate limits have yet to be explored. Due to the structure of the launcher and the use of an FR4 substrate, the transmission response in the 4.5-6 GHz band is about 5 dB lower than in the 1-3 GHz frequency range. Each dataset had a varying number of OFDM symbols in 1 frame and different transmission bandwidth. The BER and EVM are plotted against the post-overhead data rate in Figure 10.

The lower modulation orders (square marker) were error free (plotted as 10^{-8}), however, higher QAM orders produced errors. In both 64-QAM datasets, BER $< 5 \times 10^{-6}$, the 256-QAM measurements, gave a BER of 4×10^{-5} to 5×10^{-4} for 3.4 Gb/s. Comparing EVM and BER, the lower 4.9 GHz carrier frequency (blue), performed better than both 5.4 GHz and 5.7 GHz (red and yellow), as would be expected from the link's transmission response.

IV. Calibration and Extrapolation

Since the experimental results were restricted in transmission distance owing to practical constraints, here we extrapolate the maximum achievable data rates to distances which are more realistic of DSL/ADSL applications by applying a water-filling algorithm to an extrapolated channel response. The

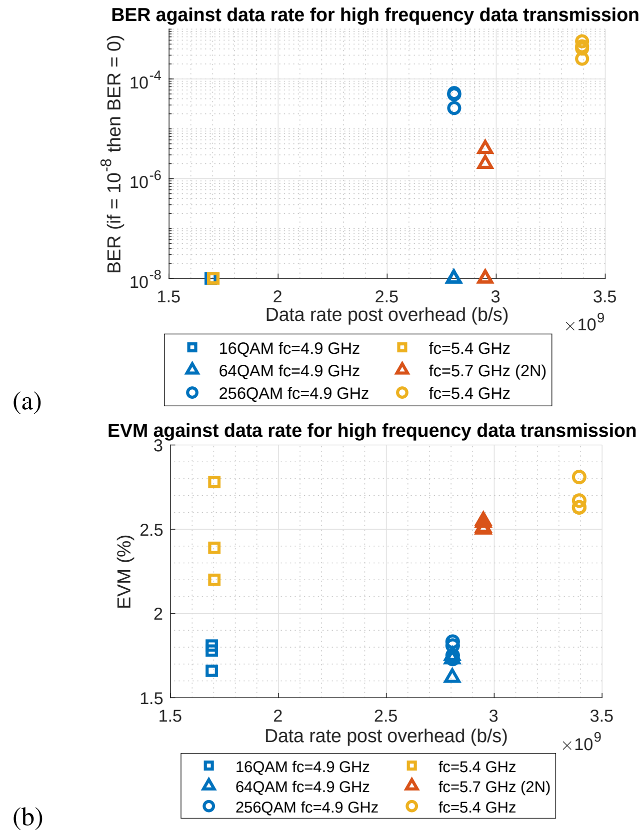

Fig. 10. (a) Bit error rate and (b) EVM for several higher carrier frequency data sets with varying modulation order (marker shape), carrier frequency (marker colour) and bandwidth represented against their data rate; 2N indicates 2 subcarrier nulls

channel response is extrapolated using measured S-parameters for DW11 cable lengths of 3 and 6 m as shown in Figure 11 (a).

As the S11 is negligible, carrying out the simple subtraction of the S21 at two cable lengths separates the launcher losses from the attenuation per unit length. A water-filling algorithm was implemented following [32] with limited power to maximise data rate. The transmission simulated includes bit loading up to 15 bit/s/Hz, a coding gain of 8.8 dB and a BER requirement $< 10^{-7}$ [17]; the full parameters are presented in the table Figure 11 (b) (unless specified otherwise in the plots).

Data rates and total power transmitted are displayed for links of various lengths in Figure 12 (a). The data rate reduces with the increasing link length as the available power saturates to its limiting value. A maximum data rate of 30.7 Gb/s is achieved up to lengths of 30 m and then starts decreasing, with predictions of 24.2 Gb/s at 50 m and 6.7 Gb/s at 100 m (higher data rates are due to the higher modulation order, up to 15 bit/s/Hz). The used power budget rapidly increases with the cable length, reaching the maximum power budget of 20 dBm at 50 m, higher power budgets will allow longer wires to transmit higher data rates (until spectral efficiency becomes the limiting factor). For example, with a power budget of 40 dBm a data rate of 16.5 Gb/s has been calculated for a 100 m DW11 cable, but surface waves' field extent may place

This article has been accepted for publication in IEEE Transactions on Communications. This is the author's version which has not been fully edited and content may change prior to final publication. Citation information: DOI 10.1109/TCOMM.2022.3190424

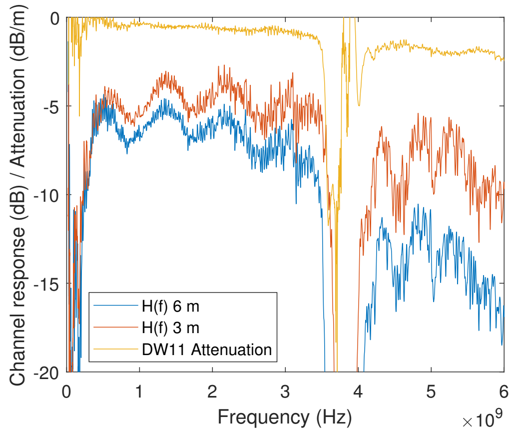

(a)

Property	Value
Carrier frequency (fc)	2.1 or 2 GHz
Bandwidth	2083 MHz
Subcarriers (Nc)	2048
Coding gain	8.8 dB
Noise margin	6dB
BER	10^{-7} (= 9.8 dB)
PSD mask	-50 dBm/Hz
Input power budget	20 dBm
Bit cap	15 bit/s/Hz
Noise floor	-150 dBm/Hz

(b)

Fig. 11. a) Measured S21 for a 3 and 6 m DW11 link and calculated attenuation in dB/m of the DW11 cable and b) Water-filling extrapolation input parameters

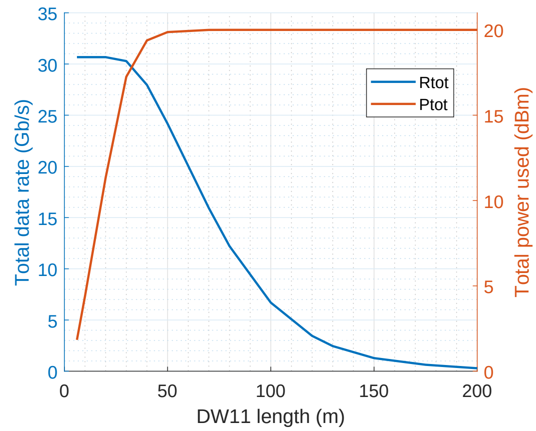

(a)

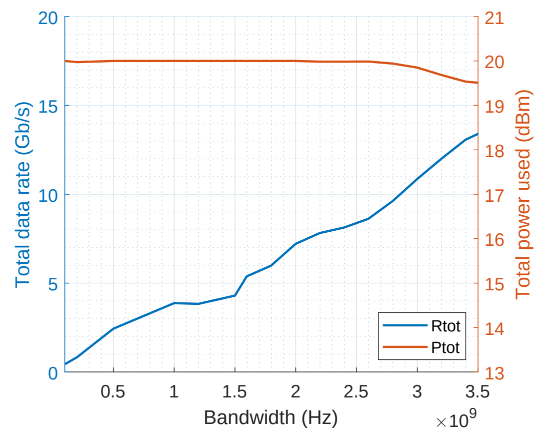

(b)

Fig. 12. a) Extrapolated data rate and transmitted power for a DW11 surface wave link against cable length and b) against transmission bandwidth for a 100 m cable

practical limits on the allowed transmit power.

Another area of interest is the relationship between data rate and transmission bandwidth. One of the main limitations of the current twisted pair technologies is the restricted operating bandwidth at longer lengths due to the cable characteristics; this is not a problem in the case of surface wave links as the frequency response is mostly defined by the launcher (at least for straight cables in free space). The relationship with fc = 2 GHz is displayed in Figure 12 (b). As expected data rate increases with available bandwidth whereas the power is capped. The bandwidth is limited by the notch in the frequency response, therefore only operating in the lower frequency range defined in Figure 5 (b) (between 0.25 and 3.75 GHz when the bandwidth is 3.5 GHz). Data rates reach 0.78 Gb/s at 200 MHz bandwidth, 3.87 Gb/s at 1 GHz, 10.85 Gb/s at 3 GHz and 13.53 Gb/s when transmitting over a 3.5 GHz wide band.

V. Conclusion

High throughput and high order modulation have been experimentally demonstrated, for the first time in literature to the authors' knowledge, to transmit data over a surface wave link. An excess of 12 Gb/s post overhead transmission over a 6.1 m standard twisted pair DW11 cable with support members has been demonstrated. A comparison with the current wired communication standard was made and scaled due to practical limits on the length of the cable which can be experimentally measured.

In this study, experimental demonstrations were carried, beyond literature's more extensive surface wave link transmission characterisation, with high-speed OFDM data transmission. Furthermore, practical implementation were considered by using widely deployed DW11 twisted pair cables and exponentially tapered planar launchers. Capacity throughput predictions were drawn from experimental link characterisation with adjustable modulation and cable length, which is novel in surface waves capacity calculations.

A data generation and processing system was implemented to measure the potential of a surface wave transmission system. Spectrally efficient modulation such as QAM and OFDM were used to allow wideband transmission with a one-tap equaliser. For clarity, channel feedback and FEC was omitted in this proof-of-concept demonstration.

A small number of transmission bit errors were observed. The prime reason for errors was a poor channel performance on particular subcarriers or interference believed from wireless transmissions (such as Wi-Fi in the 2.4 GHz ISM band). Such errors could be eliminated by nulling subcarriers or using discrete multitone modulation (DMT) provided that channel or error information is fed back to the transmitter. Furthermore, adding forward error coding and other data coding would add robustness to random errors and further decrease the system's BER.

To predict data transmission rates over longer links, the cable attenuation per metre was de-embedded allowing the extrapolation to longer length links. Furthermore, a water-filling algorithm was used to calculate the extrapolated link's ultimate capacity using multitone modulation and coding gain. A capacity of above 13 Gb/s is predicted for a 100 m DW11 cable using a bandwidth of 3.5 GHz and 20 dBm of transmit power and 24.2 Gb/s at 50 m over a 2 GHz band.

Comparatively, conventional differential mode communications on similar cables such as G.fast achieve 1 to 2 Gb/s over up to 100 m using 112 to 212 MHz bandwidths with up to 1024-QAM (10 bit/symbol) or the more recent G.mgfast achieving 5 to 10 Gb/s at 30 to 100 m [33]. Typical installations consist of large bundles of twisted pairs whereas the presented proof-of-concept experiments and extrapolation were single transmission links. Nonetheless, our measurements show that higher frequencies present a high potential with adapted launcher designs especially as they would allow much wider transmission bandwidths and therefore data throughput (in this case we presented carrier frequencies of around 5 GHz but mm-wave bands would be of high interest). The main application of this technology would therefore be dual mode excitation with surface waves as a burst mode on top of g.mgfast, and mixed mode excitation with existing differential mode transmission. Such processes would only involve a receiver implementation and be used in an opportunistic way where the network and economics of the terminals allow this to work. Further use cases could include short-range high-speed data communications, especially when considering the theoretical frequency response of surface waves as well as more manageable irregularities on the link for such applications.

While the potential of surface waves to deliver high data capacity on existing twisted pair cable infrastructure has been demonstrated, further research is required to investigate the impairments which will result from non-straight cables and external influences of the electromagnetic surface wave fields (such as large bundles), though we point out that their extent reduces with increasing carrier frequency. Studies have proven bends to be manageable at certain radii and frequencies [10], [20], [34], for more limiting cases, bend management designs [35] or surface wave repeaters could be used. The experiment also required the attachment of the conductors and strength members to the SW launcher which would complicate real world deployment. Further research would be beneficial in the area of non-intrusive launchers.

Acknowledgment

The authors would like to thank Trevor Morsman and Fraser Burton from BT for their valuable feedback on the work and the manuscript as well as providing cable samples. As well as special thanks to Prof. Mike Payne and Dr. Mayank Drolia for their input on the theoretical physics aspect of the work. Additionally we would like to acknowledge funding from BT plc, Huawei Technologies Dusseldorf GmBH, EPSRC IPES CDT (grant EP/L015455/1) and The Royal Society (grant IF170002 and INF/PHD/180021)

References

[1] R. B. Gary, "The "G-Line" Community TV System," *Radio & Television News*, pp. 40–41, nov 1956.

[2] A. Sommerfeld, "Ueber die Fortpflanzung elektrodynamischer Wellen längs eines Drahtes," *Annalen der Physik*, vol. 303, no. 2, pp. 233–290, jan 1899.

[3] G. Goubau, "Surface Waves and Their Application to Transmission Lines," *Journal of Applied Physics*, vol. 21, pp. 1119–1128, 1950.

[4] K. Wang and D. M. Mittleman, "Metal wires for terahertz wave guiding," *Nature*, vol. 432, no. November, pp. 376 – 379, 2004.

[5] T.-i. I. Jeon and D. Grischkowsky, "Direct optoelectronic generation and detection of sub-ps-electrical pulses on sub-mm- coaxial transmission lines Direct optoelectronic generation and detection of sub-ps-electrical pulses on sub-mm-coaxial transmission lines," *Applied Physics Letters*, vol. 6092, no. 2004, 2011.

[6] AT&T, "Celebrating AT&T's Project AirGig," 2019. [Online]. Available: https://about.att.com/innovationblog/2019/03/project_airgig.html

[7] J. M. Cioffi, K. J. Kerpez, C. S. Hwang, and I. Kanellakopoulos, "Terabit DSLs," *IEEE Communications Magazine*, vol. 56, no. 11, pp. 152–159, nov 2018.

[8] R. Shrestha, K. J. Kerpez, C. S. Hwang, M. Mohseni, J. M. Cioffi, and D. M. Mittleman, "A wire waveguide channel for terabit-per-second links," *Applied Physics Letters*, vol. 116, 131102, 2020.

[9] R. Shrestha, K. J. Kerpez, C. S. Hwang, M. Mohseni, J. M. Cioffi, and D. M. Mittleman, "A metal wire waveguide for terabit DSL," *International Conference on Infrared, Millimeter, and Terahertz Waves, IRMMW-TH*, sept 2020.

[10] T. Akalin, A. Treizebré, and B. Bocquet, "Single-wire transmission lines at terahertz frequencies," *IEEE Transactions on Microwave Theory and Techniques*, vol. 54, no. 6, pp. 2762–2767, 2006.

[11] M. J. King and J. C. Wiltse, "Surface-Wave Propagation on Coated or Uncoated Metal Wires at Millimeter Wavelengths," *IRE Transactions on Antennas and Propagation*, vol. 10, no. 3, pp. 246–254, 1962.

[12] Z. Wang, "Theoretical analysis of THz Sommerfeld wave propagation on metal wire at normal temperature," *Optik*, vol. 124, no. 22, pp. 5468–5472, 2013.

[13] S. J. Orfanidis, "Electromagnetic Waves and Antennas." Rutgers University New Brunswick, NJ, 2002, ch. 10, pp. 489–532.

[14] T. Schaich, D. Molnar, A. Al Rawi, and M. Payne, "Analytic modelling of a planar Goubau line with circular conductor," *Scientific Reports*, vol. 10, no. 1, p. 20754, dec 2020.

[15] K. Zhan, A. Agrawal, M. Johnson, A. Ramachandran, T. Anand, and A. Natarajan, "An integrated 7-Gb/s 60-GHz communication link over single conductor wire using sommerfeld wave propagation in 65-nm CMOS," in *IEEE MTT-S International Microwave Symposium Digest*. IEEE, jun 2017, pp. 797–800.

[16] S. Y. Kim *et al.*, "Characterization of the Goubau line for testing beam diagnostic instruments," *Journal of Instrumentation*, vol. 12, no. 12, 2017.

[17] S. Galli, J. Liu, and G. Zhang, "Bare metal wires as open waveguides, with applications to 5G," in *IEEE International Conference on Communications*, vol. 2018-May. IEEE, may 2018, pp. 1–6.

[18] British Cables Company, "Datasheet for Dropwire 11." [Online]. Available: http://britishcablescompany.com/wp-content/uploads/2019/04/BCC-Dropwire-11.pdf

[19] T. Schaich *et al.*, "Advanced Modeling of Surface Waves on Twisted Pair Cables: Surface Wave Stopbands," *IEEE Transactions on Microwave Theory and Techniques*, vol. 70, no. 5, pp. 2541–2552, 2022.

[20] J. Chiba, "Experimental Studies of the Losses and Radiations Due to Bends in the Goubau Line," *IEEE Transactions on Microwave Theory and Techniques*, vol. MTT-25, no. 2, pp. 94–100, 1977.

[21] Tektronix, "AWG70001A and AWG70002A Arbitrary Waveform Generators Installation and Safety Instructions,"

[22] Teledyne LeCroy, "Teledyne LeCroy - WavePro 804HD."

[23] D. Headland *et al.*, "Passive electric monopole array for terahertz surface wave launcher," in *IRMMW-THz 2015 - 40th International Conference on Infrared, Millimeter, and Terahertz Waves*. Institute of Electrical and Electronics Engineers Inc., nov 2015.

[24] A. Sharma, A. T. Hoang, and M. S. Reynolds, “A Coplanar Vivaldi-Style Launcher for Goubau Single-Wire Transmission Lines,” *IEEE Antennas and Wireless Propagation Letters*, vol. 16, pp. 2955–2958, 2017.

[25] R. N. Simons, *Coplanar Waveguide Circuits, Components, and Systems*, ser. Wiley Series in Microwave and Optical Engineering. Wiley, 2001.

[26] J.Armstrong, “OFDM for Optical Communications,” *Journal of Lightwave Technology*, vol. 27, no. 3, pp.189–204, 2009.

[27] T. M. Schmidl and D. C. Cox, “Robust frequency and timing synchronization for OFDM,” *IEEE Transactions on Communications*, vol. 45, no. 12, pp. 1613–1621, 1997.

[28] M. Timmers, M. Guenach, C. Nuzman, and J. Maes, “G.fast: Evolving the copper access network,” *IEEE Communications Magazine*, vol. 51, no. 8, pp. 74–79, 2013.

[29] S. M. Zafaruddin, I. Bergel, and A. Leshem, “Signal Processing for Gigabit-Rate Wireline Communications: An Overview of the State of the Art and Research Challenges,” *IEEE Signal Processing Magazine*, vol. 34, no. 5, pp. 141–164, 2017.

[30] B. Powell and E. Harstead, “FEC Selection for 25G/50G/100G EPON,” Tech. Rep., 2017.

[31] Ofcom, “Ofcom UK Spectrum Map.” [Online]. Available: http://static.ofcom.org.uk/static/spectrum/map.html

[32] T. Antonakopoulos and N. Papandreou, “Bit and power allocation in constrained multicarrier systems: The single-user case,” *Eurasip Journal on Advances in Signal Processing*, vol. 2008, pp. 14, 2008.

[33] V. Oksman *et al.*, “MGFAST: A New Generation of Copper Broadband Access,” *IEEE Communications Magazine*, vol. 57, pp. 14–21, 2019.

[34] P. Chavance and B. Chiron, “Une etude experimentale de transmission d’onde centimetriques sur guide d’ondes filiformes,” *Annales des Telecommunications*, vol. 8, pp. 367–378, 1953.

[35] D. G. Kiely, “Experiments with single-wire transmission line at 3-cm wavelength,” *Journal of the British Institution of Radio Engineers*, vol. 13, no. 4, pp. 194–199, 1953.

Ilana Toledano received her M.Eng degree in Electrical and Electronic Engineering from University College London (UCL), UK, in 2016, her M.Res in Integrated Photonics and Electronic Systems from the University of Cambridge in 2017 and her Ph.D degree in Electronic Engineering from the University of Cambridge, UK in 2021. She then joined the Cambridge University CPS group as a research associate. Her research focusses on fast copper surface waves data communications and capacity estimation through experimental work and simulations.

Syed Sheheryar Bukhari completed his PhD degree in electronics and electrical engineering from Loughborough University, UK in 2017. He worked as a research associate at Loughborough University (2017-18) and at the University of Oxford (2018-19). He was a research associate at Cavendish Labs, University of Cambridge, UK from 2019. His research interests include metasurfaces, surface waves communications and machine learning.

Ergin Dinc received his BSc degree in Electrical and Electronics Engineering from Bogazici University, Turkey, in 2012, and his Ph.D. degree in Electrical and Electronics Engineering from Koc University, Turkey in 2016. He was a postdoctoral researcher at Royal Institute of Technology (KTH), Sweden after his PhD. He was a research associate in the Internet of Everything (IoE) Group at University of Cambridge, UK between 2017-2019. Then, he joined the Cavendish Astrophysics, University of Cambridge, UK and carried out research on surface waves for high speed communication. Dr Dinc is currently working at Isotropic Systems as a Senior R&D Engineer. His research interests include ultra fast digital communications, antenna design, transformation optics and cyber-physical systems.

Tobias Schaich received the B.Sc. degree in physics from the Ludwig Maximilian University of Munich, Munich, Germany, and the M.A.St. degree in physics from the University of Cambridge, Cambridge, U.K., in 2016 and 2018, respectively, where he is currently pursuing the Ph.D. degree at the Department of Physics. His research focuses on modeling of electromagnetic surface waves on copper cables for high-speed communications.